UC San Diego
UC San Diego Previously Published Works

Title

Emissive Guanosine Analog Applicable for Real-Time Live Cell Imaging

Permalink

https://escholarship.org/uc/item/0w67h9gv

Journal

ACS Chemical Biology, 19(8)

ISSN

1554-8929

Authors

Steinbuch, Kfir B

Cong, Deyuan

Rodriguez, Anthony J

et al.

Publication Date

2024-08-05

DOI

10.1021/acschembio.4c00398

Copyright Information

Peer reviewed

Emissive Guanosine Analog Applicable for Real-Time Live Cell Imaging

Kfir B. Steinbuch, Deyuan Cong, Anthony J. Rodriguez, and Yitzhak Tor*

Cite This: https://doi.org/10.1021/acschembio.4c00398

Read Online

ACCESS | Metrics & More | Article Recommendations | Supporting Information

ABSTRACT: A new emissive guanosine analog $^{CF3th}G$, constructed by a single trifluoromethylation step from the previously reported ^{th}G, displays red-shifted absorption and emission spectra compared to its precursor. The impact of solvent type and polarity on the photophysical properties of $^{CF3th}G$ suggests that the electronic effects of the trifluoromethyl group dominate its behavior and demonstrates its susceptibility to microenvironmental polarity changes. In vitro transcription initiations using T7 RNA polymerase, initiated with $^{CF3th}G$, result in highly emissive 5′-labeled RNA transcripts, demonstrating the tolerance of the enzyme toward the analog. Viability assays with HEK293T cells displayed no detrimental effects at tested concentrations, indicating the safety of the analog for cellular applications. Live cell imaging of the free emissive guanosine analog using confocal microscopy was facilitated by its red-shifted absorption and emission and adequate brightness. Real-time live cell imaging demonstrated the release of the guanosine analog from HEK293T cells at concentration-gradient conditions, which was suppressed by the addition of guanosine.
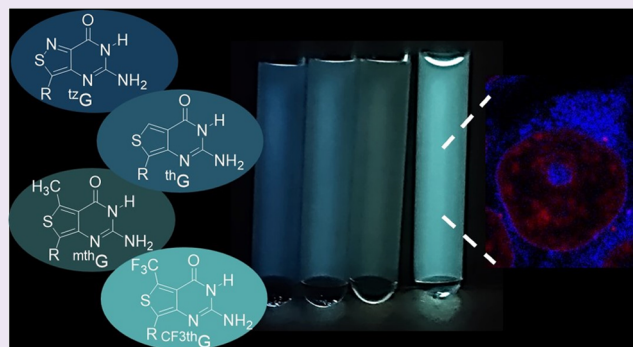
The development of fluorescent nucleoside analogs is frequently challenged by their intended applications.[1,2] Modifying the heterocyclic skeleton of the practically dark canonical purines and pyrimidines to endow them with useful photophysical features frequently renders them too perturbing.[3−5] Even surgical structural changes, such as a single atom replacement, intended to alter their photophysics, perturb both the ground and excited states, their solvation and dynamics, and their susceptibility to distinct quenching pathways, frequently in an unpredictable fashion.[6] Advancing such useful biophysical tools has therefore been an empirical and iterative process.[1,7]

While minimal alterations of the native heterocycles have yielded diverse families of useful analogs, including two emissive RNA alphabets reported by us (Figure 1), efforts are still required to expand their repertoire and application landscape.[8−11] We have recently assessed the incorporation of hydrophobic groups into the purine skeleton at the position equivalent to the purines' N7 and have hypothesized that desolvation of the Hoogsteen face may impact nonradiative decay pathways and lead to improved photophysical parameters (Figure 1).[12] We set out to test this by modifying ^{th}G, a useful and thoroughly studied fluorescent G surrogate,[10,13] by incorporating a trifluoromethyl group into its skeleton (Figure 1). Here, we report its synthesis, exploiting Baran's heteroaromatic trifluoromethylation protocol,[14,15] and evaluate its photophysical features, as well as its cellular compatibility and potential for cellular imaging.
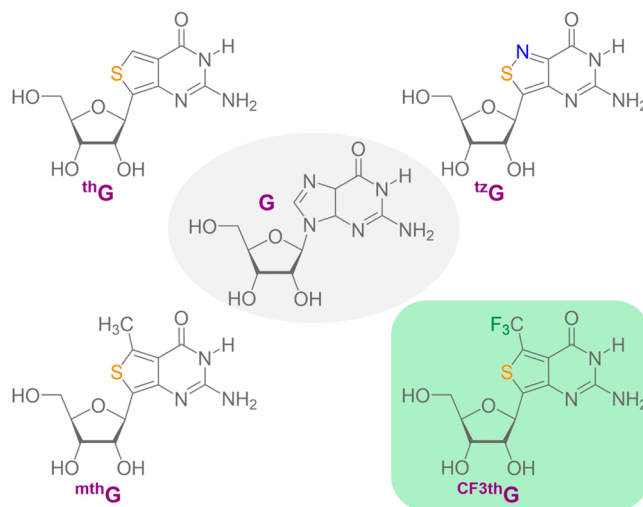
Figure 1. Guanosine and its previously reported emissive analogs, ^{th}G, ^{tz}G, ^{mth}G, and the current $^{CF3th}G$.

RESULTS AND DISCUSSION

Instead of bottom-up synthesizing the intended target nucleoside, we have opted to exploit Baran's trifluoromethylation procedures and directly modify the emissive ^{th}G.[14,15] Since rather few examples of trifluoromethylating purine-like heterocycles and nucleosides have been reported, conditions were therefore first screened, including the use of Zn vs Na trifluoromethanesulfinate salts, as well as solvent combinations and reaction temperatures (Scheme 1, SI section 1).[16] Yields

Scheme 1. Synthesis of $^{CF3th}G^a$
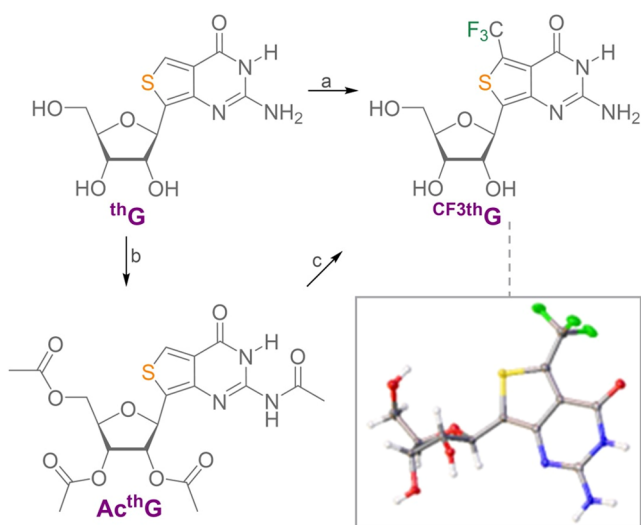
^{a}Reagents and conditions. (a) NaSO$_2$CF$_3$ 1.5 equiv, ^{t}BuOOH 1 equiv, DMSO, 18.5%. (b) Ac$_2$O, DMAP, Py, 90.0%. (c) (i) NaSO$_2$CF$_3$ or Zn(SO$_2$CF$_3$)$_2$ 3 equiv, ^{t}BuOOH 5 equiv, DMSO, 15.5%. (ii) NH$_4$OH/MeNH$_2$ 1:1, quantitative. Bottom right: crystal structure of $^{CF3th}G$.

were relatively low across the board (10−18%) but were deemed acceptable for the purpose of assessing the fundamental photophysics and utility of this new nucleoside.

X-ray crystal structure analysis of the emissive analog confirmed the β anomeric configuration and demonstrated that in the solid state, $^{CF3th}G$ displays anti orientation, as native guanosine does.[17] Overlay of the crystal structure of $^{CF3th}G$ with that of guanosine shows negligible impact of the modified nucleosbase on the sugar pucker (rmsd of 0.009 Å) and high overall similarity to the native nucleoside (rmsd 0.101 Å), including the same tautomeric preference (Figure S1).[17]

The absorption and emission spectra of the analytically and structurally characterized $^{CF3th}G$, as well as their sensitivity to changes in polarity and pH, were recorded (Figure 2, Table 1). Both the absorption and emission maxima of $^{CF3th}G$ in water (343 and 475 nm, respectively) were red-shifted compared to ^{th}G (Figure 2a and Table 1).[10] Unlike the complex spectra displayed by ^{th}G, due to its ground-state tautomerization,[18] $^{CF3th}G$ displays simpler spectra suggesting one predominant tautomer. The emission spectrum of ^{th}G displays a maximum and a shoulder that peak at 453 and 400 nm, respectively, when excited at its absorption maximum at 321 nm (Figure S2).[10] This is due to the presence of two ground-state tautomers H-1 and H-3, which could also be selectively excited (Figure S2).[18] The emission spectrum of $^{CF3th}G$ is simpler and displays only a small shoulder below 400 nm, suggesting a minimal contribution from a minor tautomer. To test this hypothesis, emission spectra
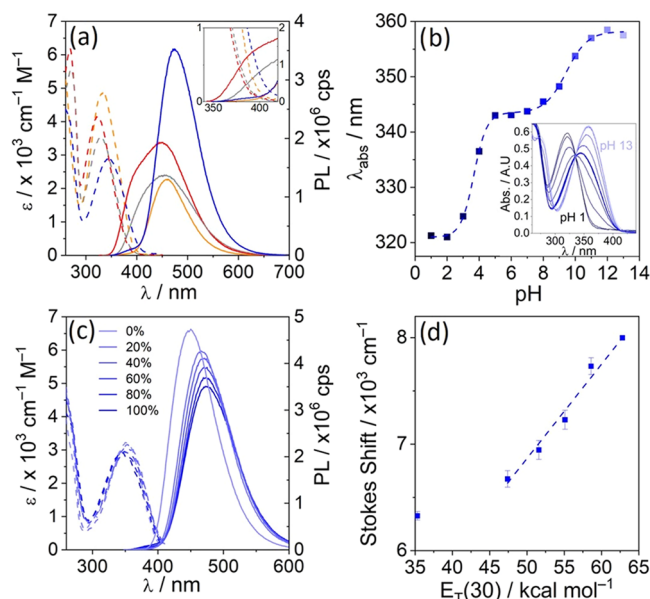
Figure 2. (a) Absorption (dashed lines) and emission (solid lines) spectra of ^{tz}G (orange), ^{th}G (red), ^{mth}G (gray), and $^{CF3th}G$ (blue) in water; inset: expansion of Abs/em around 400 nm demonstrating $^{CF3th}G$ still absorbs above 400 nm, which could facilitate its visualization in confocal microscopy using 405 nm excitation; (b) absorption maxima variation of $^{CF3th}G$ versus pH, inset: absorption spectra of $^{CF3th}G$ at pH 1 (black) to 13 (light blue); (c) absorption (dashed lines) and emission (solid lines) spectra of $^{CF3th}G$ in water (blue), dioxane (light blue), and mixture thereof (80, 60, 40, and 20% v/v water in dioxane); (d) Stokes shift correlation versus solvent polarity (E$_T$(30)) of water/dioxane mixtures for $^{CF3th}G$ with standard errors. Note: the data point at 35.3 kcal mol^{-1} (100% dioxane) was excluded from the linear fit. Emission intensities were corrected to reflect an optical density of 0.1 at λ_{max}. All photophysical measurements were performed in at least three replicates.

excited at higher and lower energies were recorded. Excitation at higher energy (310 nm) resulted in a second emission peak with a maximum of around 384 nm, while excitation at lower energy (390 nm) resulted in a spectrum that aligns with the emission spectrum of $^{CF3th}G$ when excited at its absorption maximum (343 nm) (Figure S2). This suggests the presence of two ground-state tautomers in solution, with the H-1 $^{CF3th}G$ being the dominant one, as inferred from the observations made for ^{th}G.[18]

While its extinction coefficient is lower, the higher emission quantum yield of $^{CF3th}G$ (ϕ = 0.54) results in comparable brightness to the parent nucleoside ^{th}G as well as to ^{tz}G and ^{mth}G (Table 1).[10−12] Compared to spectra taken in water, batho- and hyperchromic shifts were observed for absorption spectra of $^{CF3th}G$ in dioxane, and hypso- and hyperchromic shifts were observed for the emission maxima (Table 1), associated with a slightly higher emission quantum yield (ϕ = 0.61). To determine its ground-state pK_a values, absorption spectra of $^{CF3th}G$ were recorded in buffered solutions at pH 1−13 (Figure 2b). By fitting a double Boltzmann sigmoidal curve to the plot of absorption maxima vs pH, two pK_a values of 3.7 and 9.4 were extracted. As expected, these values are lower than those of ^{th}G and ^{mth}G and are closer to the more isomorphic analog ^{tz}G due to the electron-withdrawing inductive effect of the trifluoromethyl group.[10−12]

Sensitivity to microenvironmental polarity was determined by measuring the absorption and emission of $^{CF3th}G$ in water/

Table 1. Photophysical Data for Emissive Guanosine Analogs

	solvent	λ_{abs} $[\varepsilon]^a$	λ_{em} $[\Phi]^a$	$\Phi\varepsilon$	Stokes shift^a	polarity sensitivity^b	pK_a^{c}
^{tz}G	water	333 (4.9)	459 (0.25)	1203	8.27	102.0	3.55, 8.51
	dioxane	339 (4.7)	425 (0.17)	539	6.01		
thG	water	321 (4.1)	453 (0.46)	1909	9.58	107.2	4.4, 10.3
	dioxane	333 (4.5)	424 (0.50)	2265	6.89		
^{mth}G	water	327 (3.5)	456 (0.42)	1470	8.70	130	5.0, 10.4
	dioxane	334 (3.6)	443 (0.61)	2200	7.20		
^{CF3th}G	water	343 (2.9)	475 (0.54)	1566	8.10	89	3.66, 9.44
	dioxane	354 (3.3)	450 (0.61)	2013	6.02		

$^a\lambda_{abs}$, λ_{em}, ε, and Stokes shifts are reported in nm, nm, 10^3 M^{-1} cm^{-1}, and cm^{-1}, respectively. All photophysical values reflect the average of at least three independent measurements. ^{b}Sensitivity to polarity, expressed in cm^{-1}/(kcal mol^{-1}), is equal to the slope of the linearization depicted in Figure 2d. ^{c}pK_a values are equal to the inflection points determined by the fitting curve in Figure 2b. Values for ^{tz}G, thG, and ^{mth}G were taken from refs 10−11, respectively. See Table S3 for data including experimental errors for ^{CF3th}G.

dioxane mixtures (Figure 2c). Correlating the observed Stokes shifts vs Reichardt's $E_T(30)$ parameters (Figure 2d) shows comparable behavior to our other emissive guanosine analogs (Table 1).[19]

To study the effect the CF$_3$ moiety has on the photophysics of ^{CF3th}G, spectra were taken in trifluoroethanol (TFE) and compared to other alcohols and water. Stokes shifts of ^{CF3th}G in the different alcohols and water were plotted against their $E_T(30)$ values[20] and against their hydrogen-bond strength α_1 parameter[21] (Figure S3, Table S5). The linear correlations observed show that no solvent-specific effects impact the photophysics of ^{CF3th}G (Figure S3b,c, Table S5). To further probe this matter, the absorption and emission spectra of ^{CF3th}G in H$_2$O vs D$_2$O were compared[22] and were found nearly identical (Figure S4). These results, therefore, further suggest that the inductive electronic effect of the CF$_3$ moiety is dominating the photophysics of ^{CF3th}G over its environmental- and solvent-specific effect.

The ability of ^{CF3th}G, as a free nucleoside, to initiate in vitro transcription reactions using T7 RNA polymerase was evaluated and compared to GTP (Figure 3).[23−25] Using the nucleoside and not the nucleotide facilitates the generation of strands labeled only at the 5′ position.[26] Transcripts obtained were separated by PAGE and visualized under UV light. For the in vitro transcription reaction containing ^{CF3th}G, bands corresponding to GTP initiation (T1) and ^{CF3th}G initiation (T2) were visible by UV shadowing. The latter band was also fluorescent and hence visible upon illumination at 365 nm (Figures 3 and S5).[27,28] The extracted transcripts were characterized by their emission spectra and MALDI-TOF MS analyses, supporting their assigned sequences (Figure 3). The desired, highly emissive ^{CF3th}G-initiated strand was quantified by its absorption at 260 nm and was found to be in ∼8-fold excess of the corresponding template DNA duplex. Its relative yield, compared to that of the native transcript formed in the same transcription reaction, was 0.38.

To probe the imaging potential of ^{CF3th}G, its cytotoxicity and cellular uptake were first evaluated. MTT cell viability assay demonstrated that ^{CF3th}G, as well as the other analogs, ^{mth}G, thG, ^{tz}G, and the native guanosine, did not have a detrimental effect on the cell viability of HEK293T cells up to the highest tested concentration (500 μM) after 24 h incubation (Figure S6).[29]

Following calibration and optimization experiment using widefield microscopy (Figures S8 and S9), confocal imaging illustrated that ^{CF3th}G could be clearly visualized in live HEK293T cells using a 405 nm laser excitation, while ^{mth}G, thG, and ^{tz}G could not be detected (Figures 4a and S10). ^{CF3th}G
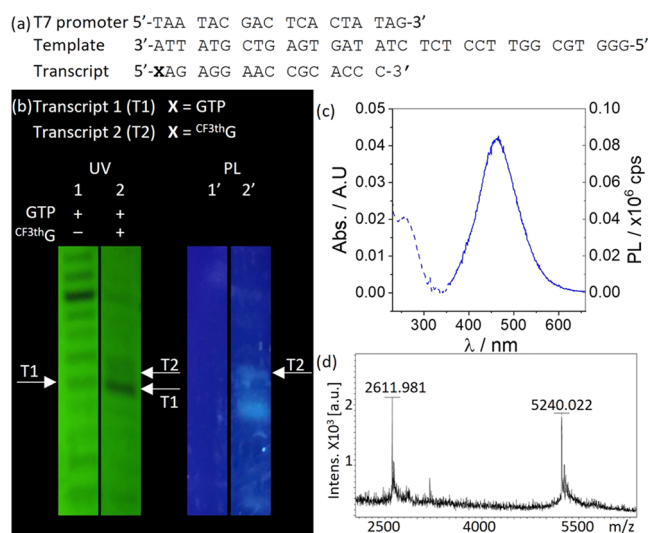

Figure 3. Transcription reactions with the T7 RNA polymerase. (a) T7 promoter and template strand sequences; (b) transcription reaction using the template with 2 mM of all-natural NTPs, with or without ^{CF3th}G (10 mM). The white arrows indicate the target native transcript, T1, and the ^{CF3th}G-initiated transcripts, T2. UV shadowing and photoluminescence (PL) were observed upon illumination at 254 and 365 nm, respectively; (c) absorption (dashed line) and emission (solid line) of T2; (d) MALDI-TOF mass spectrum of transcript T2.

was observed in the nucleus and the cytosol. In the nucleus, it appeared to localize into spherical structures, perhaps the nucleolus, where the synthesis of ribosomes takes place.[30] In the cytosol, most of the signal by ^{CF3th}G adopted a distinct pattern spreading throughout the cell rather than a uniformly diffused signal. To determine if ^{CF3th}G colocalizes with certain cellular organelles, cells incubated with ^{CF3th}G were also stained with lyso-tracker, Mito-tracker, ER-tracker, and lipid droplet markers (Figure S11). Results show that the pattern of ^{CF3th}G moderately colocalizes with the ER, with a Pearson colocalization factor of 0.35 (Figure 4b, SI section 5.4).[31] The Mander's colocalization coefficients indicate that the signal of ^{CF3th}G is found in the ER and the lysosomes, as their fractions of signals overlapping with the signal of ^{CF3th}G are 0.999 and 0.98, respectively (Figure 4b, SI section 5.4).[31]

Finally, real-time live cell imaging of ^{CF3th}G over the course of 30 min captured the movements of ^{CF3th}G in the cells as well as its expulsion (Figure 5a, Sup Movie 1). It was hypothesized that ^{CF3th}G could be expelled from the cells due to concentration gradients as the samples were washed, and an imaging medium
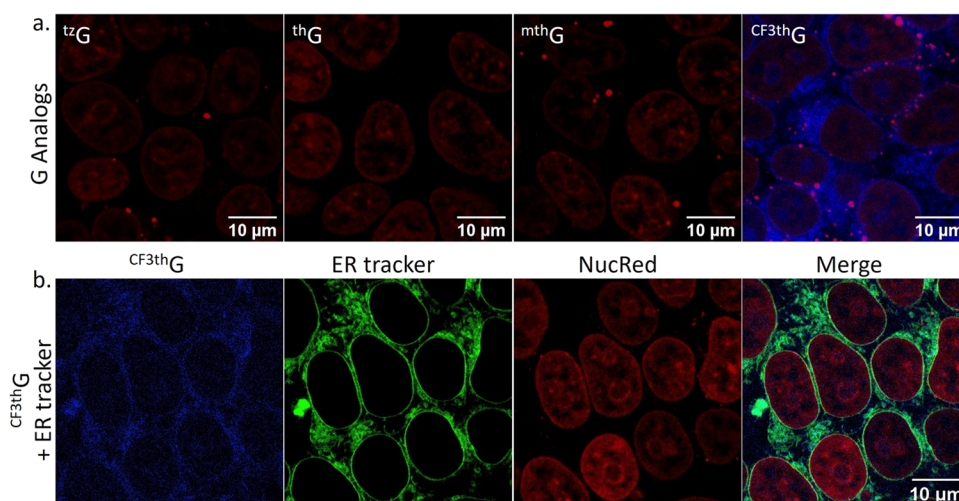
Figure 4. Live cell imaging of HEK293T incubated with (a) ^{tz}G, thG, ^{mth}G, or ^{CF3th}G (500 μM) for 24 h (merged channels); (b) ^{CF3th}G (500 μM) for 24 h and stained with an ER-tracker for 30 min. To visualize the cells, nuclei were stained with NucRed for 30 min. Figure 4 represents the results of at least two independent experiments.
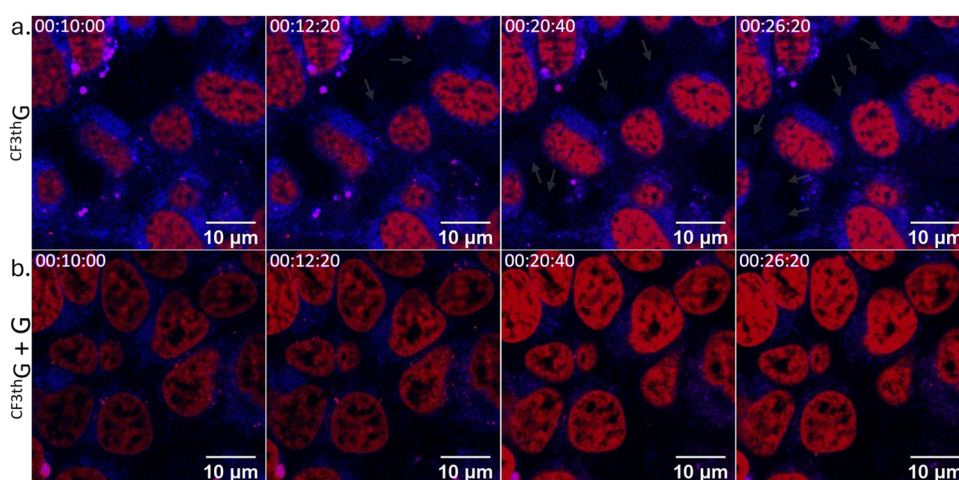
Figure 5. Real-time live cell imaging of HEK293T cells incubated with ^{CF3th}G (500 μM) for 24 h. After incubation, cells were washed twice and visualized in Fluorobrite (a) or Fluorobrite supplemented with guanosine (500 μM) (b) for 30 min. Nuclei were stained with NucRed. The experiment's results were reproduced in two independent experiments.

was applied prior to microscopic visualization. An identical experiment in which native guanosine (500 μM) was added to the imaging media supported this hypothesis, as cellular ^{CF3th}G was better retained over 30 min (Figure 5b, Sup Movie 2). Exosomal release of guanosine by muscle satellite cells, which could be delivered to the central nervous system has been previously reported.[32,33] While additional experimentation is necessary, it is plausible that ^{CF3th}G is capable of visualizing endogenous phenomena associated with the release of guanosine derivatives via exosomes.

In summary, we introduce ^{CF3th}G, a new emissive guanosine analog, synthesized by direct trifluoromethylation of thG or ActhG based on Baran's trifluoromethylation methods. T7 RNA polymerase was found to initiate in vitro transcription with ^{CF3th}G, resulting in highly emissive 5′-end-tagged RNA transcripts, suggesting that the new emissive analog, despite its large Hoogsteen face substituent, can still be recognized by polymerases. While other emissive nucleosides have been recently reported to facilitate live cell imaging, it appears that these analogs could be visualized only when embedded into RNA strands.[34−36] Here, we demonstrate that due to its intense

visible emission, ^{CF3th}G can be visualized as the free nucleoside in live mammalian cells and could be monitored in real time. Imaging experiments with and without guanosine allude to its similarity to guanosine. Further studies, however, are needed to support that the physicochemical differences between ^{CF3th}G and G do not significantly alter the nucleoside's cellular biochemistry, localization, and metabolism. Having a guanosine-like probe that can be visualized while being taken and released from the cells, as shown here, could potentially assist in shedding light on cellular processes involving guanosine.[37−40]

■ METHODS

General Chemistry Methods. Reagents, buffers, and salts were purchased from Sigma-Aldrich, Fluka, TCI, Acros, Synchem, Inc. (Elk Grove, IL), and were used without further purification unless otherwise specified. NTPs were purchased from Fisher. Template and promoter oligonucleotides were purchased from IDT. T7 RNA polymerase (P266L) was expressed and purified as previously reported.[25]

Solvents were purchased from Sigma-Aldrich and Fisher Scientific and dried by standard techniques. NMR solvents were purchased from Cambridge Isotope Laboratories (Andover, MA). All reactions were monitored with analytical TLC (Merck Kieselgel 60 F$_{254}$). All

D

experiments involving air and/or moisture-sensitive compounds were carried out under an argon atmosphere. Column chromatography was carried out with a silica gel particle size of 40−63 μm. NMR spectra were obtained on Bruker AVA 300 MHz, Varian Mercury 400 MHz, and Varian VX 500 MHz. MALDI-TOF mass spectra were obtained on a Bruker Autoflex Max MALDI-TOF-MS. ESI-TOF mass spectra were obtained on an Agilent 6230 HR-ESI-TOF MS instrument at the Molecular Mass Spectrometry Facility at the UCSD Chemistry and Biochemistry Department.

General Photophysics Methods. Spectroscopic grade DMSO and dioxane were obtained from Sigma-Aldrich, and aqueous solutions were prepared with Milli-Q deionized water. All measurements were carried out in a 1 cm, four-sided quartz cuvette from Helma. All measurements were reproduced in at least 3 independent experiments.

Absorption spectra were measured on a Shimadzu UV-2450 spectrophotometer, setting the slit at 1 nm and using a resolution of 0.5 nm. All spectra were corrected for the blank. Steady-state emission spectra were measured on a Horiba Fluoromax-4 instrument setting the excitation and the emission slits at 1 and 3 nm, respectively, and the resolution at 1 nm. Both instruments were equipped with a thermostat-controlled ethylene glycol water bath fitted to a specially designed cuvette holder, and the temperature was kept at 25.00 ± 0.10 °C. All spectra were corrected for the blank.

Nucleosides (^{tz}G, thG, ^{mth}G, and ^{CF3th}G) were dissolved in DMSO to prepare highly concentrated stock solutions (10 mM). In a typical experiment, aliquots were diluted into solvents to a final volume of either 125 μL or 3 mL.

Cell Biology and Confocal Microscopy. HEK293T cells were grown in DMEM supplemented with 10% FCS and 1% penicillin-streptomycin. Cells were grown in a humidified chamber with 95% air and 5% CO_2 at 37 °C. 96-well microtiter plates and Fluorodish wells were coated with PDL before use according to the following procedure: Wells were covered with PDL solution (0.1 mg mL^{-1}, 100 or 120 μL per well for 96-well plate or fluorodish well, respectively) and incubated for 3 h at RT. The PDL solution was then removed by aspiration, and wells were resterilized under UV light for 20 min and further dried for an additional 1.5 h. Wells were finally washed twice with PBS (100 or 120 μL per well).

Live cell imaging was performed using a Nikon AXR confocal microscope with four lines (405, 488, 561, and 640 nm) LUA-S4 laser engine and DUX-VB detector using bandpass and long-pass filter for each channel (420−551, 655−850 nm) mounted on a Nikon Ti2 using an Apo 100 × 1.45 NA objective and operated using NIS elements 5.42.03 software. Image stacks were acquired in Galvano mode in unidirectional scanning with a 405 nm laser at 3% power and 61.5 μm pinhole size and 640 nm laser at 2% power and 61.0 μm pinhole size at a frame size of 1024 × 1024 at scan zoom 1.7. Cells were maintained at 37 °C and 5% CO_2 with 80% humidity using an okolab bold line.

■ ASSOCIATED CONTENT

ⓢ Supporting Information

The Supporting Information is available free of charge at https://pubs.acs.org/doi/10.1021/acschembio.4c00398.

Synthetic procedures; photophysical data; in vitro transcription; cell biology; and fluorescence microscopy protocols; movies of real-time imaging timelapse (PDF)

Sup Movie 1 (ZIP)

Sup Movie 2 (ZIP)

■ AUTHOR INFORMATION

Corresponding Author

Yitzhak Tor − *Department of Chemistry and Biochemistry, University of California, San Diego, California 92093-0358, United States;* ◉ orcid.org/0000-0003-3726-7799; Email: ytor@ucsd.edu

Authors

Kfir B. Steinbuch − *Department of Chemistry and Biochemistry, University of California, San Diego, California 92093-0358, United States*

Deyuan Cong − *Department of Chemistry and Biochemistry, University of California, San Diego, California 92093-0358, United States*

Anthony J. Rodriguez − *Department of Chemistry and Biochemistry, University of California, San Diego, California 92093-0358, United States*

Complete contact information is available at:
https://pubs.acs.org/10.1021/acschembio.4c00398

Author Contributions

The manuscript was written through contributions of all authors. All authors have given approval to the final version of the manuscript.

■ ABBREVIATIONS

PAGE, poly(acrylamide gel electrophoresis); MTT, 3-(4,5-dimethylthiazolyl-2)-2, 5-diphenyltetrazolium bromide; ER, endoplasmic reticulum; ActhG, per-acetylated thG; TFE, trifluoroethanol

■ REFERENCES

(1) Tor, Y. Isomorphic Fluorescent Nucleosides. *Acc. Chem. Res.* **2024**, *57*, 1325−1335.

(2) Dziuba, D. Environmentally Sensitive Fluorescent Nucleoside Analogues as Probes for Nucleic Acid - Protein Interactions: Molecular Design and Biosensing Applications. *Methods Appl. Fluoresc.* **2022**, *10* (4), 044001.

(3) Xu, W.; Chan, K. M.; Kool, E. T. Fluorescent Nucleobases as Tools for Studying DNA and RNA. *Nat. Chem.* **2017**, *9* (11), 1043−1055.

(4) Sinkeldam, R. W.; Greco, N. J.; Tor, Y. Fluorescent Analogs of Biomolecular Building Blocks: Design, Properties, and Applications. *Chem. Rev.* **2010**, *110* (5), 2579−2619.

(5) de Moliner, F.; Nadal-Bufi, F.; Vendrell, M. Recent Advances in Minimal Fluorescent Probes for Optical Imaging. *Curr. Opin. Chem. Biol.* **2024**, *80*, No. 102458.

(6) Dziuba, D.; Didier, P.; Ciaco, S.; Barth, A.; Seidel, C. A. M.; Mély, Y. Fundamental Photophysics of Isomorphic and Expanded Fluorescent Nucleoside Analogues. *Chem. Soc. Rev.* **2021**, *50* (12), 7062−7107.

(7) Steinbuch, K. B.; Tor, Y. Isomorphic Fluorescent Nucleoside Analogs. In *Handbook of Chemical Biology of Nucleic Acids*; Springer Nature Singapore: Singapore, 2023; pp 1−24.

(8) Jones, A. C.; Neely, R. K. 2-Aminopurine as a Fluorescent Probe of DNA Conformation and the DNA-Enzyme Interface. *Q. Rev. Biophys.* **2015**, *48* (2), 244−279.

(9) Da Costa, C. P.; Fedor, M. J.; Scott, L. G. 8-Azaguanine Reporter of Purine Ionization States in Structured RNAs. *J. Am. Chem. Soc.* **2007**, *129* (11), 3426−3432.

(10) Shin, D.; Sinkeldam, R. W.; Tor, Y. Emissive RNA Alphabet. *J. Am. Chem. Soc.* **2011**, *133* (38), 14912−14915.

(11) Rovira, A. R.; Fin, A.; Tor, Y. Chemical Mutagenesis of an Emissive RNA Alphabet. *J. Am. Chem. Soc.* **2015**, *137* (46), 14602−14605.

(12) Ludford, P. T.; Yang, S.; Bucardo, M. S.; Tor, Y. A New Variant of Emissive RNA Alphabets. *Chem. - Eur. J.* **2022**, *28* (13), No. e2021044.

(13) Kuchlyan, J.; Martinez-Fernandez, L.; Mori, M.; Gavvala, K.; Ciaco, S.; Boudier, C.; Richert, L.; Didier, P.; Tor, Y.; Improta, R.; Mély, Y. What Makes Thienoguanosine an Outstanding Fluorescent DNA Probe? *J. Am. Chem. Soc.* **2020**, *142* (40), 16999−17014.

(14) Fujiwara, Y.; Dixon, J. A.; O'hara, F.; Funder, E. D.; Dixon, D. D.; Rodriguez, R. A.; Baxter, R. D.; Herlé, B.; Sach, N.; Collins, M. R.; Ishihara, Y.; Baran, P. S. Practical and Innate Carbon Hydrogen Functionalization of Heterocycles. *Nature* **2012**, *492* (7427), 95−99.

(15) Ji, Y.; Brueckl, T.; Baxter, R. D.; Fujiwara, Y.; Seiple, I. B.; Su, S.; Blackmond, D. G.; Baran, P. S. Innate C-H Trifluoromethylation of Heterocycles. *Proc. Natl. Acad. Sci. U.S.A.* **2011**, *108* (35), 14411−14415.

(16) Chrominski, M.; Baranowski, M. R.; Chmielinski, S.; Kowalska, J.; Jemielity, J. Synthesis of Trifluoromethylated Purine Ribonucleotides and Their Evaluation as 19F NMR Probes. *J. Org. Chem.* **2020**, *85* (5), 3440−3453.

(17) Thewalt, U.; Bugg, C. E.; Marsh, R. E. The Crystal Structure of Guanosine Dihydrate and Inosine Dihydrate. *Acta Crystallogr., Sect. B: Struct. Crystallogr. Cryst. Chem.* **1970**, *26* (8), 1089−1101.

(18) Sholokh, M.; Improta, R.; Mori, M.; Sharma, R.; Kenfack, C.; Shin, D.; Voltz, K.; Stote, R. H.; Zaporozhets, O. A.; Botta, M.; Tor, Y.; Mély, Y. Tautomers of a Fluorescent G Surrogate and Their Distinct Photophysics Provide Additional Information Channels. *Angew. Chem., Int. Ed.* **2016**, *55* (28), 7974−7978.

(19) Reichardt, C. Solvatochromic Dyes as Solvent Polarity Indicators. *Chem. Rev.* **1994**, *94* (8), 2319−2358.

(20) Islam, M. R.; Warsi, F.; Khan, A. B.; Kausar, T.; Khan, I.; Ali, M. Solvatochromism of Binary Mixtures of 2,2,2-Trifluoroethanol + Ionic Liquid [Bmim][Tf2N]: A Comparative Study with Molecular Solvents. *J. Chem. Eng. Data* **2019**, *64* (3), 1140−1154.

(21) Laurence, C.; Mansour, S.; Vuluga, D.; Sraïdi, K.; Legros, J. Theoretical, Semiempirical, and Experimental Solvatochromic Comparison Methods for the Construction of the α1 Scale of Hydrogen-Bond Donation of Solvents. *J. Org. Chem.* **2022**, *87* (9), 6273−6287.

(22) Stryer, L. Excited-State Proton-Transfer Reactions. A Deuterium Isotope Effect on Fluorescence. *J. Am. Chem. Soc.* **1966**, *88* (24), 5708−5712.

(23) Milligan, J. F.; Groebe, D. R.; Witherell, G. W.; Uhlenbeck, O. C. Oligoribonucleotide Synthesis Using T7 RNA Polymerase and Synthetic DNA Templates. *Nucleic Acids Res.* **1987**, *15* (21), 8783−8798.

(24) Milligan, J. F.; Uhlenbeck, O. C. Synthesis of Small RNAs Using T7 RNA Polymerase. *Methods Enzymol.* **1989**, *180*, 51−62.

(25) Lyon, S.; Gopalan, V. A T7 RNA Polymerase Mutant Enhances the Yield of 5′-Thienoguanosine-Initiated RNAs. *ChemBioChem* **2018**, *19* (2), 142−146.

(26) Li, Y.; Fin, A.; McCoy, L.; Tor, Y. Polymerase-Mediated Site-Specific Incorporation of a Synthetic Fluorescent Isomorphic G Surrogate into RNA. *Angew. Chem., Int. Ed.* **2017**, *56* (5), 1303−1307.

(27) For both transcription reactions, as previously seen for this template (ref 28.), higher molecular weight transcripts are formed as well, containing additional nucleotides. For fuller analysis of the gel see SI Section 4.

(28) Cong, D.; Li, Y.; Ludford, P. T.; Tor, Y. Isomorphic Fluorescent Nucleosides Facilitate Real-Time Monitoring of RNA Depurination by Ribosome Inactivating Proteins. *Chem. - Eur. J.* **2022**, *28* (35), e202200994 DOI: 10.1002/chem.202200994.

(29) Mosmann, T. Rapid Colorimetric Assay for Cellular Growth and Survival: Application to Proliferation and Cytotoxicity Assays. *J. Immunol. Methods* **1983**, *65*, 55−63.

(30) Boisvert, F. M.; Van Koningsbruggen, S.; Navascués, J.; Lamond, A. I. The Multifunctional Nucleolus. *Nat. Rev. Mol. Cell Biol.* **2007**, *8* (7), 574−585.

(31) Mcdonald, J. H.; Dunn, K. W. Statistical Tests for Measures of Colocalization in Biological Microscopy. *J. Microsc.* **2013**, *252* (3), 295−302.

(32) Pietrangelo, T.; Di Filippo, E. S.; Locatelli, M.; Piacenza, F.; Farina, M.; Pavoni, E.; Di Donato, A.; Innosa, D.; Provinciali, M.; Fulle, S. Extracellular Guanosine 5′-Triphosphate Induces Human Muscle Satellite Cells to Release Exosomes Stuffed with Guanosine. *Front. Pharmacol.* **2018**, *9*, 152.

(33) Pietrangelo, T. Raising the Guanosine-Based Molecules as Regulators of Excitable Tissues by the Exosomal-Vehiculated Signaling. *Front. Pharmacol.* **2021**, *12*, 658370.

(34) Wang, D.; Shalamberidze, A.; Arguello, A. E.; Purse, B. W.; Kleiner, R. E. Live-Cell RNA Imaging with Metabolically Incorporated Fluorescent Nucleosides. *J. Am. Chem. Soc.* **2022**, *144* (32), 14647−14656.

(35) Baladi, T.; Nilsson, J. R.; Gallud, A.; Celauro, E.; Gasse, C.; Levi-Acobas, F.; Sarac, I.; Hollenstein, M. R.; Dahlén, A.; Esbjörner, E. K.; Wilhelmsson, L. M. Stealth Fluorescence Labeling for Live Microscopy Imaging of MRNA Delivery. *J. Am. Chem. Soc.* **2021**, *143* (14), 5413−5424.

(36) Nilsson, J. R.; Benitez-Martin, C.; Sansom, H. G.; Pfeiffer, P.; Baladi, T.; Le, H. N.; Dahlén, A.; Magennis, S. W.; Wilhelmsson, L. M. Multiphoton Characterization and Live Cell Imaging Using Fluorescent Adenine Analogue 2CNqA. *Phys. Chem. Chem. Phys.* **2023**, *25* (30), 20218−20224.

(37) G related processes have been demonstrated to play a role in different physiological and pathological conditions (refs 38−40).

(38) Molz, S.; Dal-Cim, T.; Budni, J.; Martín-de-Saavedra, M. D.; Egea, J.; Romero, A.; del Barrio, L.; Rodrigues, A. L. S.; López, M. G.; Tasca, C. I. Neuroprotective Effect of Guanosine against Glutamate-Induced Cell Death in Rat Hippocampal Slices Is Mediated by the Phosphatidylinositol-3 Kinase/Akt/ Glycogen Synthase Kinase 3β Pathway Activation and Inducible Nitric Oxide Synthase Inhibition. *J. Neurosci. Res.* **2011**, *89* (9), 1400−1408.

(39) Dal-Cim, T.; Poluceno, G. G.; Lanznaster, D.; de Oliveira, K. A.; Nedel, C. B.; Tasca, C. I. Guanosine Prevents Oxidative Damage and Glutamate Uptake Impairment Induced by Oxygen/Glucose Deprivation in Cortical Astrocyte Cultures: Involvement of A1 and A2A Adenosine Receptors and PI3K, MEK, and PKC Pathways. *Purinergic Signalling* **2019**, *15* (4), 465−476.

(40) Di Iorio, P.; Beggiato, S.; Ronci, M.; Nedel, C. B.; Tasca, C. I.; Zuccarini, M. Unfolding New Roles for Guanine-Based Purines and Their Metabolizing Enzymes in Cancer and Aging Disorders. *Front. Pharmacol.* **2021**, *12*, 653549.